Magneto-photoconductivity of three dimensional topological insulator bismuth telluride

Cao, Bingchen; Eginligil, Mustafa; Yu, Ting

2018

Cao, B., Eginligil, M., & Yu, T. (2018). Magneto-photoconductivity of three dimensional topological insulator bismuth telluride. Journal of Physics: Conference Series, 969, 012149-. doi:10.1088/1742-6596/969/1/012149

https://hdl.handle.net/10356/88127

https://doi.org/10.1088/1742-6596/969/1/012149

Magneto-photoconductivity of three dimensional topological insulator bismuth telluride

Bingchen Cao[1], Mustafa Eginligil[2*], Ting Yu[1]

[1] Division of Physics and Applied Physics, School of Physical and Mathematical Sciences, Nanyang Technological University, 637371, Singapore
[2] Key Laboratory of Flexible Electronics (KLOFE) & Institute of Advanced Materials (IAM), Jiangsu National Synergetic Innovation Center for Advanced Materials (SICAM), Nanjing Tech University (NanjingTech), 30 South Puzhu Road, Nanjing 211816, China

[*] iameginligil@njtech.edu.cn

Abstract. Magnetic field dependence of the photocurrent in a 3D topological insulator is studied. Among the 3D topological insulators bismuth telluride has unique hexagonal warping and spin texture which has been studied by photoemission, scanning tunnelling microscopy and transport. Here, we report on low temperature magneto-photoconductivity, up to 7 T, of two metallic bismuth telluride topological insulator samples with 68 and 110 nm thicknesses excited by 2.33 eV photon energy along the magnetic field perpendicular to the sample plane. At 4 K, both samples exhibit negative magneto-photoconductance below 4 T, which is as a result of weak-antilocalization of Dirac fermions similar to the previous observations in electrical transport. However the thinner sample shows positive magneto-photoconductance above 4 T. This can be attributed to the coupling of surface states. On the other hand, the thicker sample shows no positive magneto-photoconductance up to 7 T since there is only one surface state at play. By fitting the magneto-photoconductivity data of the thicker sample to the localization formula, we obtain weak antilocalization behaviour at 4, 10, and 20 K, as expected; however, weak localization behaviour at 30 K, which is a sign of surface states masked by bulk states. Also, from the temperature dependence of phase coherence length bulk carrier-carrier interaction is identified separately from the surface states. Therefore, it is possible to distinguish surface states by magneto-photoconductivity at low temperature, even in metallic samples.

1. Introduction

Topological insulator (TI) is an exotic phase of quantum matter with an insulating bulk state as well as time-reversal symmetry-protected Dirac-like surface states. The materials having TI phase belong to a large family of material systems ranging from 2D to 3D and from HgTe quantum wells to bismuth, selenium, tellurium, and antimony based alloys [1]. Well-known examples of bismuth based TI materials are bismuth selenide (Bi_2Se_3) and bismuth telluride (Bi_2Te_3) which are 3D TI for thickness above 5 nm (5 quintuples) [2]. One of the intriguing differences between these two similar tetradymite type structure 3D TI systems, is the unconventional hexagonal warping of the surface states in Bi_2Te_3 [3] which is the reason behind the observations of snowflake shape of the Fermi surface in angle resolved photoemission spectroscopy [4] and surface band oscillations in scanning tunnelling

microscopy [5]. A rich spin texture is a natural expectation of the warping of the surface states. In order to make use of the spin properties of TI systems, as a first step, the conduction of surface states shouldn't be masked by bulk conduction. Although Bi_2Te_3 is usually rather metallic and the Fermi energy is way above the Dirac point, it is possible to make Bi_2Te_3 non-metallic and Shubnikov-de Haas (SdH) oscillations can be observed; which is a clear sign of the surface state conduction as shown at low temperature transport studies [6]. Another transport feature of TI materials is the weak-antilocalization (WAL) observed as a negative magneto-conductance in Bi_2Te_3 thin films [7] due to the absence of backscattering by nonmagnetic impurities [8]. At high magnetic fields, the WAL is suppressed. In magneto-transport of 3D Bi_2Te_3, a detailed and careful analysis is required to extract information about surface state conduction. In these two transport signatures, the SdH oscillations and the WAL, distinguishing bulk conduction from surface state conduction remains as a challenge.

On the other hand, opto-electronic response of the surface states can be obtained from helicity-dependent photocurrents by using circularly polarized light [9]. As demonstrated in 250 nm thick 3D TI Bi_2Se_3, the sign of spin-dependent photocurrent changes based on light helicity as a result of circular photogalvanic effect (CPGE) acting on the helical Dirac surface states [10]. This shows the importance of photocurrent studies in TI to identify the surface state conduction. The CPGE can also be observed at normal incidence if a magnetic field is applied [9]. Therefore it is possible to observe surface state conduction by photocurrent at non zero magnetic field. The photo-excited carriers in the surface states can couple with the magnetic field and there will be a net photocurrent which has magnetic field dependence. In this work, we present low temperature magneto-photoconductance (MPC) of two 3D Bi_2Te_3 samples, with different thickness, excited by polarized light with a normal incidence on to the sample plane and the magnetic field applied in the illumination direction. We show that even at zero degree angle of photon polarization it is possible to distinguish surface states from bulk states by MPC and provide a discussion in terms of localization effects. Then we further elaborate the temperature dependence of MPC in the thicker sample which shows unexpected localization behaviour. We interpret this observation in terms of separation of surface state conduction from bulk conduction.

2. Experimental

Exfoliated flakes of Bi_2Te_3 were fabricated into four terminal devices. Two samples were picked for MPC measurements, with thickness 68 nm (S1) and 110 nm (S2) as determined by AFM measurements. The current voltage (IV) characteristics and the laser power dependence of photocurrent of the two samples are similar and comparable to the previously reported ones [11]. Figure 1(a) and (b) shows the IV at room and 4 K, and photocurrent at various laser powers at 4 K, respectively, for S1.

Measurements are performed in a cryostat with a micrometer precision stage. After locating the devices, IV is performed by four probe technique. The measured linear IV indicates the contacts are ohmic. Then, a beam spot of 1 micron is focused at the center of the two electrodes separated by 2 microns. A linearly polarized solid state laser with wavelength 532 nm chopped by 137 Hz frequency and the magnitude and phase of photocurrent signal are collected by a low noise current pre-amplifier connected to a lock-in amplifier. A quarter waveplate is set initially to zero degree photon polarization. Photocurrent is measured for laser powers lying in the linear response regime. The magnetic field is applied perpendicular to the sample plane.
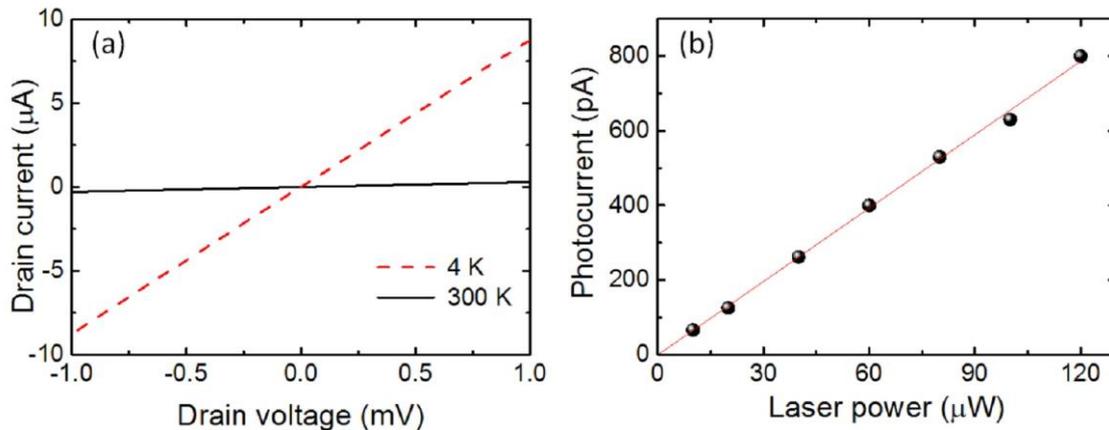
Figure 1 (a) IV characteristics of sample 1 (S1) and (b) photocurrent as a function of incident laser for S1. The photocurrent response is linear with laser power.

3. Results and discussion

3.1. Laser power and thickness dependence of the MPC

In Fig. 2(a) the laser power dependence of the MPC of the thinner sample, S1 for 80 and 120 µW laser powers at 4 K is given., The MPC behaviors at two different laser powers are similar and based on the linear dependence of photocurrent of Fig. 1(b), it seems to be proportional at all fields. There is a negative MPC up to 4 T, which turns to a positive MPC at higher fields. The negative MPC is qualitatively similar to the previously observed WAL in transport [7]. As the field increases, the negative MPC is suppressed by spin-dependent transport term due to the surface states since there are no magnetic impurities in the system. But also, as the 3D quantum limit is exceeded at high fields [12] and two surface states can be coupled as the thickness get smaller [13], it is possible to observe a positive MPC. This turnover from negative MPC to positive MPC at 4 T, agrees well with the previous transport in low carrier density Bi_2Se_3 [12].
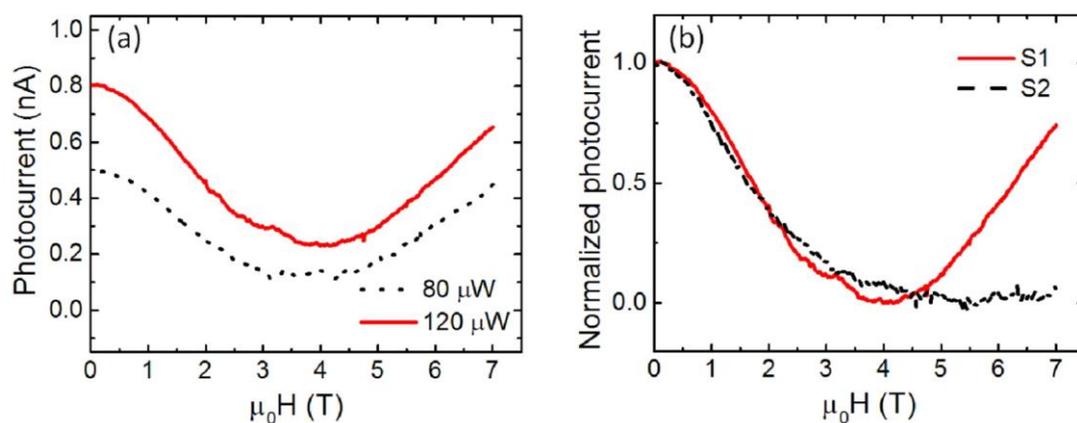

Figure 2. (a) Photocurrent of thinner sample S1 shown at two different laser power (b) normalized photocurrent at 120 µW of two samples are compared. The MPC of the thinner sample dramatically changes sign around 4 T, while thicker sample becomes constant.

While S1 exhibits a turnover as a function of field and several photocurrent contributions take place; the thicker sample, S2, exhibits a simple negative MPC behavior. In Fig. 2(b), the photocurrent values of S1 and S2 at 4 K and 120 µW laser power are compared. The photocurrent value of S1 at

zero field (4 T) is taken as 1 (0) and the photocurrent value of S2 at zero field (5.5 T) is taken as 1 (0). The negative MPC in S2 seems to saturate around 5.5 T. But at higher fields, it looks like constant rather than a positive MPC. This could be due to the increase in the ratio of bulk state conduction to surface state conduction as the thickness of TI increases. Since there is no positive MPC at higher fields, one can think that there is only one surface state at play and the analysis of the thicker sample S2 can be simpler. Similar to magneto-transport, this effect can be taken as WAL effect and useful parameters can be extracted.

3.2. Temperature dependence of MPC

The magnitude of negative MPC of S2 drops as temperature increases as seen in Fig.3. There are some fluctuations of MPC, which may remind the Aharanov-Bohm oscillations observed in topological insulator nanoribbons for in-plane magnetic fields [14]. On the other hand, S1 doesn't seem to have these fluctuations. As S2 is twice as thick, there could be contribution from the side surface states coupling with magnetic field. Although there is no clear trend in the fluctuations in S2, they are up to 10 pA. Given the fact that the change in photocurrent as a function of time at zero field within half an hour is not more than 1 pA, these fluctuations are not only noise. This need to be further studied in a different setup in which the applied field can be varied from perpendicular to the sample plane to in-plane.
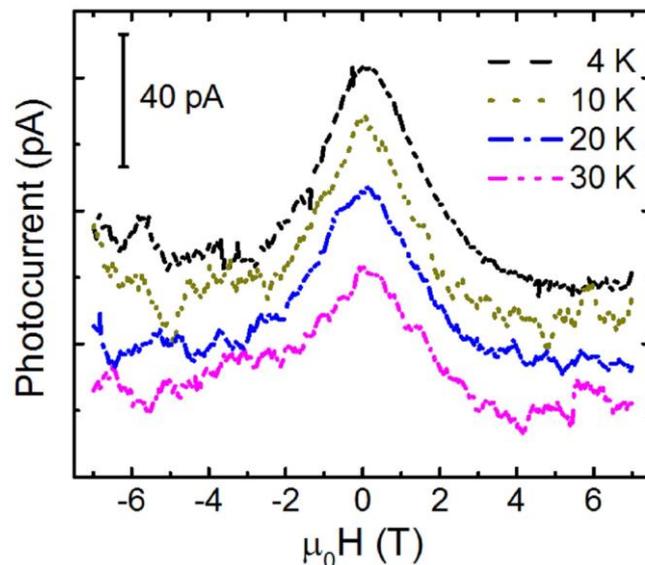

Figure 3. Temperature dependence of MPC at several temperatures shown.

The temperature dependent MPC data can be fit to localization formula [15] for photocurrent as follows,

$$\Delta PC = -\frac{\alpha e^2}{2\pi^2\hbar}\left[ln\frac{\hbar}{4Bel_\phi^2} - \psi\left(\frac{1}{2} + \frac{\hbar}{4Bel_\phi^2}\right)\right]$$

where e is the electronic charge, $\hbar$ is the Planck's constant, l_ϕ is the phase coherent length, and ψ is the digamma function, α should be equal to 1 and -1/2 for the orthogonal and symplectic cases, respectively. The fitting in Fig. 4(a) yields, α = -0.65, -0.56, -0.32, and 0.26 at 4 K, 10 K, 20 K, and 30 K, respectively. If α is -1/2 there should be one surface state, if it is equal to -1 there should be two surface states involved in the conduction of this strong spin-orbit coupling system. At temperatures below 20 K, there seems to be one surface state contributing to the conduction, which also explains why there is no positive MPC at higher fields. As temperature increases α drops because the surface

state conduction becomes smaller. Eventually, at 30 K, there is a sign change of α which indicates, bulk states completely mask the surface states conduction.
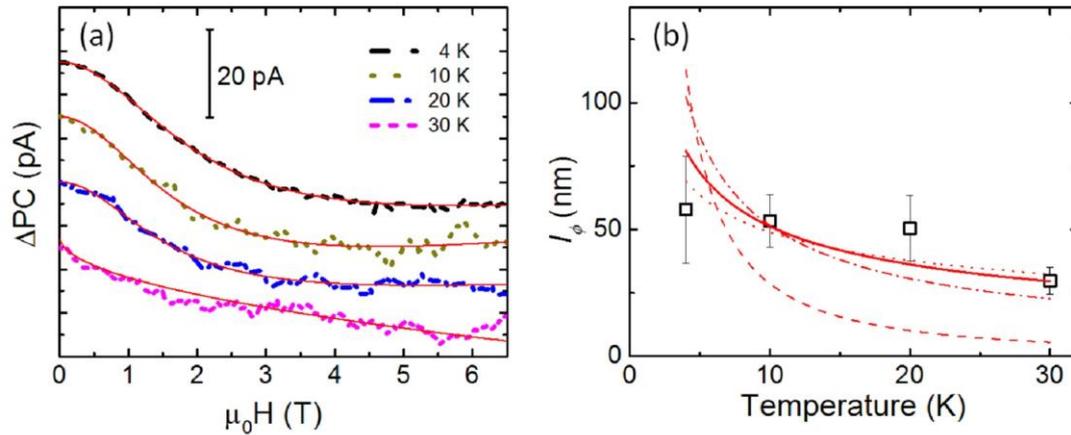

Figure 4. (a) The difference between the photocurrent PC at a field and the PC at zero field, ΔPC, as a function of magnetic field at several temperatures is given, the curves are repositioned for a better presentation, the red solid lines are the localization fittings (b) phase coherence lengths plotted against temperature and fitted to $T^{-p/2}$ for p = 0.75 (dot), 1 (solid), 1.5 (dash dot), and 3 (dash).

In Figure 4(b) the phase coherence lengths l_ϕ that are extracted from the localization fitting are plotted. The temperature dependence of $l_\phi \sim T^{-\frac{p}{2}}$ can provide information about the carrier-carrier (p = 3/2) or carrier-phonon interactions (p=3) [16]. Several possible fittings are shown: p=3 (dash) seems to be worse; while p=0.75 (dot) and 1 (solid) are better ones (which have no physical meaning), p=1.5 (dash dot) is a better fit than p=3. This may indicate the electron-electron interaction, which is due to the bulk carriers may also play a role at low temperatures. This means in addition to weak-antilocalization due to the surface states, bulk state conduction can be identified by carrier-carrier interaction [17]. However, there is only one data point under 10 K and this data point deviates from the expectation of p=1.5 curve. Therefore there is a need for more data points less than 10 K to have a better understanding of this MPC feature.

4. Summary and conclusion

Briefly, this work presents the difference in magneto-photoconductivity behavior of two metallic 3D Bi_2Te_3 samples with different thickness for 2.33 eV linearly polarized excitation with zero photon polarization. A negative MPC for both samples at fields lower than 4 T can be understood as WAL similar to transport. At higher fields, 68 nm thick sample shows positive MPC due to the coupling of surface states. The 110 nm thick sample shows photocurrent due to one surface state and as shown by the localization fitting analysis of MPC data at several temperatures, bulk conduction can be identified separately. This demonstrates another way to identify surface states, in addition to the photocurrent at zero magnetic field and oblique incidence. Similarly, the control over surface states by MPC can be studied by right and left circularly polarized excitations, as well as wavelength dependence of MPC.

References

[1] Yan B, and Zhang S-C, *Rep. Prog. Phys.* **75**, 096501 (2012).
[2] Zhang Y *et al.*, *Nat. Phys.* **6** 584–588 (2010).
[3] Fu L *Phys.Rev. Lett.* **103**, 266801 (2009).
[4] Chen Y L *et al.*, *Science* **325**, 178 (2009).
[5] Alpichshev Z *et al.*, *Phys.Rev. Lett.* **104**, 016401 (2010).
[6] Qu D-X, Hor Y S, Xiong J, Cava R J, and Ong N P, *Science* **329**, 821 (2010).
[7] He H-T *et al.*, *Phys.Rev. Lett.* **106**, 166805 (2011).
[8] Zhang T *et al.*, *Phys.Rev. Lett.* **103**, 266803 (2009).
[9] Hosur P, *Phys.Rev. B* **83**, 035309 (2011).
[10] McIver J M, Hsieh D, Steinberg H, Jarillo-Herrero P, and Gedik N, *Nat. Nanotechnol.* **7**, 96 (2012).
[11] Yao J D, Shao J M, Li S W, Bao D H, and Yang G W, *Sci. Reports* **5**, 14184 (2015).
[12] Analytis J G, McDonald R D, Riggs S C, Chu J-H, Boebinger G S, and Fisher I R, *Nat. Phys.* **6**, 960-964 (2010).
[13] Akiyama R, Fujisawa K, Sakurai R, and Kuroda S, *Journal of Physics: Conference Series*, **568**, 052001 (2014).
[14] Peng H, *Nat. Mater.* **9**, 225 (2010).
[15] Hikami S, Larkin A I, and Nagaoka Y, *Prog. Theor. Phys.* **63**, 707 (1980).
[16] Lu H-Z, AND Shen S-Q, *Front. Phys*. **12**(3), 127201 (2017).
[17] Wang J *et al*., Phys. Rev. B **83**, 245438 (2011)